J Mater Sci (2016) 51:3971–3978
DOI 10.1007/s10853-015-9715-4

Iron-doping effects on the CO_2 tolerance of a perovskite oxygen permeable membrane

Xia Tang[1] · Xingxing Zhang[1] · Wei Luo[1] · Chengzhang Wu[1] · Yuwen Zhang[1] · Weizhong Ding[1] · Chenghua Sun[2]

Received: 26 October 2015 / Accepted: 30 December 2015 / Published online: 8 January 2016

Abstract $Ba_{0.8}La_{0.2}Co_{0.88-x}Fe_xNb_{0.12}O_{3-\delta}$ membranes (BLCFN) with different Fe-doping were successfully prepared by solid-state reaction method. The microstructure, oxygen permeability, thermal analysis, and oxygen permeation stability using CO_2 as sweep gas were systematically investigated. After being calcined under pure CO_2, BLCFN membranes remain their major perovskite phase but diffraction peaks of $BaCO_3$, CoO appeared on the membranes which Fe content is less than 0.2. Apparent activation energy of oxygen permeation are around 60–70 kJ/mol for all membranes. With the increase of Fe-doping content, the flux through BLCFN membranes decreases but the degradation of oxygen flux becomes less pronounced when CO_2 is used as sweep gas at 850 °C. Enhanced CO_2 resistance of the perovskite would be resulted from an increasing average binding energy due to the Fe-doping. For the membrane where the Fe-doped content equals to 0.2, the oxygen permeation flux is 0.96 mL cm^{-2} min^{-1} at 900 °C with He sweeping. When using pure CO_2 as sweep gas, the oxygen permeation flux decreases slightly in the first 50 h and then reaches a steady state of $\sim$0.31 mL cm^{-2} min^{-1} for more than 60 h in a prolonged continuous oxygen operation. The observations indicated that a stable oxygen permeation could be realized by suitable elemental doping in a single perovskite membrane.

✉ Chengzhang Wu
wucz@shu.edu.cn

[1] State Key Laboratory of Advanced Special Steel, Shanghai University, Shanghai 200072, China

[2] School of Chemistry, Monash University, Clayton, VIC 3800, Australia

Introduction

As a kind of green-house gas, carbon dioxide has been attracting great attention worldwide in view of its effect on global climate change [1]. CO_2 capture from coal-fired power plants via oxy-fuel process is gaining prominence [2]. Utilization of mixed ionic and electronic conducting membranes (MIECM) for the oxygen production becomes popular in the past decades due to the oxygen separation using MIECM with infinite selectivity and low cost [3, 4]. For a practical application in the Integrated Gasification Combined Cycle (IGCC) system, both high performance and chemical stability to CO_2 are required for the MIECM. However, it is well-acknowledged that perovskite ceramics containing alkaline earth elements are susceptible to CO_2 attack [5, 6]. Therefore, to explore the CO_2-tolerant oxygen transport membranes is a practical requirement of developing oxy-fuel IGCC system.

Nowadays, some oxygen transport membranes with CO_2 tolerance have been explored, e.g., $La_2NiO_{4+\delta}$ type materials [7] or dual-phase materials [8]. However, the oxygen permeation flux of these membranes is still limited. Normally, MIECM with $ABO_{3-\delta}$ perovskite structure exhibits high oxygen flux, whereas, perovskite ceramics have been found vulnerable to the presence of CO_2. For instance, when the membranes of $Ba_{0.5}Sr_{0.5}Co_{0.8}Fe_{0.2}O_{3-\delta}$ [5] and $BaCo_{0.4}Fe_{0.4}Nb_{0.2}O_{3-\delta}$[6] suffered an oxygen permeation process with pure CO_2 as sweep gas, a complete breakdown of the oxygen permeation flux was observed within a few minutes. A way to stabilize the perovskite structure is via proper cation substitution, i.e., doping less reactive elements on the A- and/or B-site [7, 8]. Chen et al. and Zeng et al. doped SCF materials with 10 % tantalum [7] or 10 % titanium [8], which greatly improves tolerance towards CO_2. Yi et al. studied the effect of CO_2 exposure

on sweep side for $BaCo_{1-x-y}Fe_xNb_yO_{3-\delta}$ membrane after the fully substitution of Co by Fe and Nb in the B-site, and found the $BaFe_{0.8}Nb_{0.2}O_{3-\delta}$ membrane shows no carbonate formation but very low oxygen permeation [9]. In addition, the authors compared the CO_2 tolerance of membranes of $SrFe_{0.8}Nb_{0.2}O_{3-\delta}$ and $BaFe_{0.8}Nb_{0.2}O_{3-\delta}$ and found that the former one shows the better CO_2-tolerant properties [10]. At 900 °C, a considerable oxygen flux of 0.25 mL cm^{-2} min^{-1} was achieved for a 1.0 mm thick $SrFe_{0.8}Nb_{0.2}O_{3-\delta}$ membrane, which is remained steady at this value in a prolonged measurement running for over 210 h. Additionally, the elemental substitution of rare-earth metal like La on the A-site of perovskite could improve the tolerance towards CO_2 too [11, 12]. The 1.0 mm thick $La_{0.6}Sr_{0.4}Co_{0.8}Fe_{0.2}O_{3-\delta}$ membrane achieved an oxygen permeation flux of 0.1 mL cm^{-2} min^{-1} and was stable in pure CO_2 atmosphere for the investigated period of over 200 h continuous operation [11].

Recently, we found that a permeation flux of 2.61 mL cm^{-2} min^{-1} can be obtained through $BaCo_{0.9}Nb_{0.1}O_{3-\delta}$ (BCN) membrane at 900 °C under the Air/He gradient [13]. On the basis of the high oxygen flux BCN material, we prepared $Ba_{o.8}La_{0.2}Co_{0.88}Nb_{0.12}O_{3-\delta}$ (BLCN) membrane by doping La element on the A-site of BCN material. The BLCN membrane shows improved tolerance against CO_2 as compared to the BCN membrane. La-doping was found to be accorded with an increase of average binding energy (ABE), which leads to the enhanced CO_2 resistance [12].

Therefore, whatever rare-earth element is doped in A-site or transition elements are doped in B-site, the tolerance towards CO_2 might be improved. Particularly, the membrane of $SrFe_{0.8}Nb_{0.2}O_{3-\delta}$ has totally tolerance towards CO_2, which indicated that, even for the membrane with alkaline earth metal fully occupied in A-site, carbonate formation can also be restricted through a suitable element doping in B-site. Inspired by this point, in this study, BLCN membrane was chosen as a target membrane material, the oxygen permeability, and structural stability of the Fe-doped BLCN membranes were investigated under He/CO_2 atmosphere. The results show that the Fe-doped BLCN membranes are CO_2 tolerant and possess high oxygen permeability.

Materials and methods

Preparation of membranes

$Ba_{o.8}La_{0.2}Co_{0.88-x}Fe_xNb_{0.12}O_{3-\delta}$ (BLCFN, $x = 0$, 0.1, 0.2, 0.3 and 0.5) powder was prepared by solid-state reaction method which described in our previous work [14]. Stoichiometric amounts of $BaCO_3$, La_2O_3, Co_3O_4, Fe_3O_4, and Nb_2O_5 (AR grade) were mixed by wet-milling for 48 h with zirconia balls in ethanol. After fully mixed and dried, the powders were calcined at a temperature range of 1040–1190 °C for 12 h to obtain the perovskite phase (the higher Fe content is, the higher temperature is needed). The calcined BLCFN powders were ball-milled for 36 h again and then dried. After that, the powders were pressed into disks under a pressure of ~110 MPa and then sintered at 1170–1270 °C for 8 h to get dense membranes. According to the Fe-doping content, as-prepared membranes were abbreviated as BLCFN-0.0, BLCFN-0.1, BLCFN-0.2, BLCFN-0.3, and BLCFN-0.5, respectively.

Measurement of oxygen permeation

Silver rings were used to seal BLCFN membranes in a thickness of 1.0 mm at 850 °C for permeation test. The effective area of the membranes for oxygen permeation is ca. 1.3 cm^2. Synthetic air was used as feed gas and He or CO_2 was used as sweep gas. Air was introduced into the feed side with a flow rate of 110 ml/min and He or CO_2 with a flow rate of 80 ml/min was swept on the permeate side. The composition of the permeated effluent gas was determined by gas chromatography (Varian CP-3800), and the oxygen permeation flux was calculated based on the following equation [13]:

$$J_{O_2} = (C_{O_2} - C_{N_2} \times \frac{21}{79}) \times \frac{F_{He}}{A}, \quad (1)$$

where C_{O_2} and C_{N_2} are measured oxygen and nitrogen concentrations in the gas on the permeate side, respectively, and F_{He} is the flow rate of permeate stream (ml/min) and A is the active membrane area (cm^2). The leakage was no more than 1.0 % for all the oxygen permeation experiments.

Characterization of the membranes materials

The phase structure of the membranes was determined by X-ray diffraction (XRD, Rigaku DLMAX-2200, Cu Kα). Datasets were recorded at room temperature in a 2θ range of 10–90° with a step width of 0.02°. The thermal stability of the material was studied by TG/DSC (Netzsch STA449 F3). The surface and cross section of membranes were studied by scanning electron microscopy (SEM) using a SEM (HITACHI SU-1510) at a voltage of 15 kV.

Results and discussion

Microstructural analysis

BLCFN membranes were examined by XRD measurement and XRD patterns of the membranes are shown in Fig. 1. It

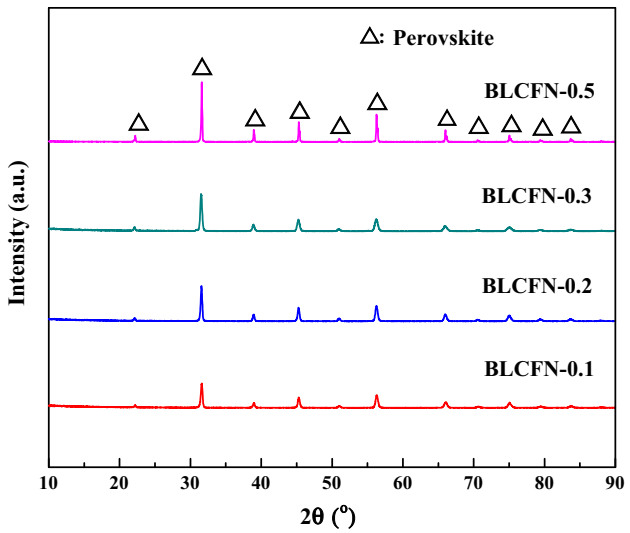

Fig. 1 XRD patterns of as-synthesized BLCFN powders

can be seen that all the calcined BLCFN membranes with different Fe content display just perovskite cubic structure. Figure 2 presents SEM images of the prepared BLCFN membrane after being sintered at 1170, 1180, 1190, 1270 °C. We can find that BLCFN grains are distributed very uniformly and the boundaries are clear in the membrane, no typical intergranular fractured microstructure with grains are visible. The grain sizes are in the range of 5–10 μm.

Carbonates are easily formed when the perovskite oxides containing alkaline earth metal are exposed to a CO_2 atmosphere [15]. The decomposition and formation temperature of the carbonates depend on the partial pressure of CO_2 and stability of the perovskite structure [5]. To test the stability of the BLCFN membranes in an atmosphere of CO_2, the membranes were firstly calcined under pure CO_2 at 850 °C for 5 h and 20 h, respectively, and then the phase structures were identified by XRD. As shown in Fig. 3, all the membranes calcined in pure CO_2 for 5 h remain their major perovskite phase. However, diffraction peaks of $BaCO_3$ appeared on the BLCFN-0.0, BLCFN-0.1, and BLCFN-0.2 membranes. In addition, CoO was also identified by XRD for the membranes which Fe content is less than 0.2. Moreover, it can be seen that the peaks intensity of carbonate decreases with the increase of Fe in B-site, suggesting that the Fe-doped BLCN membranes are more stable in CO_2 atmosphere. While the calcination time under CO_2 is prolonged to 20 h, as shown in Fig. 3b, phase structure of BLCFN membranes did not change significantly comparing with the membrane treated in a short time of 5 h. There are minor carbonate formation in the membrane of BLCFN-0.2 and BLCFN-0.3, and no carbonate formation in the BLCFN-0.5 membrane. The results are consistent with the observation in SEM images. Surfaces morphology of BLCFN-0.0, BLCFN-0.1, and BLCFN-0.5 membranes calcined in pure CO_2 for 5 h and 20 h, are shown in Fig. 4. For the membrane of BLCFN-0.0, i.e., no Fe-doping, the precipitation of carbonate can be observed in the grain boundaries (Fig. 4a and b), which was also proven by EDX analysis. The relative elemental distribution of metallic cations of Ba:La:Co:Nb in the fresh

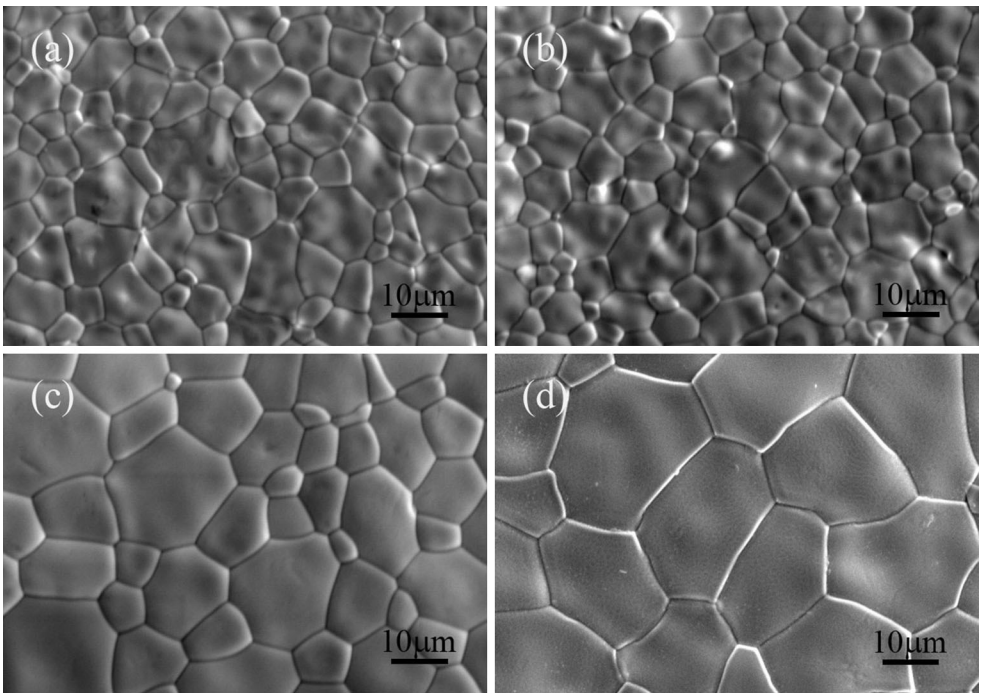

Fig. 2 SEM images of as-synthesized BLCFN membranes. **a** BLCFN-0.1, **b** BLCFN-0.2, **c** BLCFN-0.3, **d** BLCFN-0.5

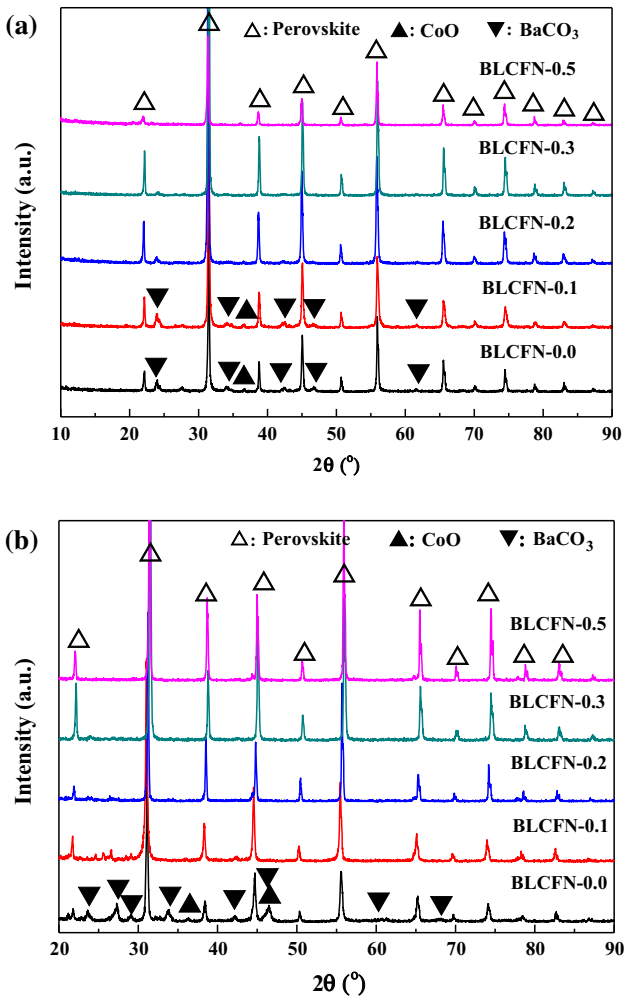

Fig. 3 XRD patterns of BLCFN membranes after calcining at 850 °C under pure CO_2 for 5 h (**a**) and 20 h (**b**). $BaCO_3$: JCPDS 41-0373; CoO: JCPDS 43-1004; Perovskite: JCPDS 46-0997

BLCFN-0.0 sample should be 80:20:88:12. Whereas, after calcination for 5 h in CO_2, the elemental distribution in the grain boundaries becomes to 80:6.1:12.2:1.4, suggesting that the Ba enrichment in the zone of grain boundaries. For the Fe-doped BLCFN membrane, it can be seen that Fe-doping further restricts the reaction of the membrane and CO_2 (Fig. 4c–f). Particularly, when Fe content reaches 0.5, there is no obvious carbonate formation even suffering the calcination under pure CO_2 for 20 h (Fig. 4f).

Thermal analysis

The Fe-doped BLCFN samples exhibited an excellent resistance to CO_2 corrosion in comparison of the BLCN membrane without Fe-doping. In order to obtain a quantitative analysis of the weight change of BLCFN samples under CO_2-containing atmosphere, thermal analysis method was applied and the results are shown in Fig. 5. It can be found that the weight change profiles of BLCFN samples with different proportions of Fe-doping are similar. At the initial stage, the weight of samples decreases very slightly, which is due to the remove of the impurities adsorbed on the surface of the samples. Then the samples exhibited an obvious weight loss around 500 °C. As we know, there should be two tendencies in the case of perovskite oxide upon heating in CO_2-containing atmosphere: on one hand, BLCFN powders upon heating under an atmosphere of low oxygen partial pressure (CO_2/N_2) would result in a loss of lattice oxygen (known as α-O_2 and β-O_2) due to the reduction of transition metal cations; on the other hand, the reaction of alkaline earth metal cation, lattice oxygen, and carbon dioxide happens, e.g., $Ba^{2+} + O^{2-} + CO_2 \rightarrow BaCO_3$. The former tendency will lead to a weight loss but the latter one will result in a weight gain. According to the above analysis, the weight loss around 500 °C indicated that the loss of the lattice oxygen is dominant effect in comparison of carbonate formation.

Temperature dependence of oxygen permeation

Figure 6 shows the temperature dependence of the oxygen permeability of the BLCFN membranes and the related Arrhenius plots. Here, all of the oxygen permeation data were collected after reaching steady state. As shown in Fig. 6a, the oxygen flux for all membranes increases with the elevated temperature as expected. Obviously, perovskite BLCFN-0.0 membrane has higher oxygen flux than all other membrane with Fe-doping at each temperature, and the flux through BLCFN membranes decreases with the increase of Fe-doping content. At 900 °C, oxygen permeation flux reaches 1.29, 1.16, 0.82, 0.59, and 0.32 mL min^{-1} cm^{-2} for BLCFN-0.0, BLCFN-0.1, BLCFN-0.2, BLCFN-0.3, and BLCFN-0.5, respectively. In addition, according to the temperature dependence of oxygen flux through the membranes, apparent activation energy (E_a) can be obtained from Arrhenius plots shown in Fig. 6b. Specifically, the values of E_a were calculated to be 67.5, 62.6, 70.5, 75.1, and 65.2 kJ mol^{-1} for the BLCFN membranes with increasing Fe-doping content, respectively.

Time dependence of oxygen permeation

Whatever from the XRD patterns of the membrane after the calcination in CO_2 atmosphere or TG results of the BLCFN samples upon heating in a flowing CO_2-containing atmosphere, we can find that the Fe-doping enhances the CO_2 tolerance properties of membranes. In order to better understand the oxygen permeability of BLCFN after Fe-doping in B-site, the oxygen permeation flux of BLCFN membranes was tested with pure CO_2 sweeping, and the results are shown in Fig. 7.

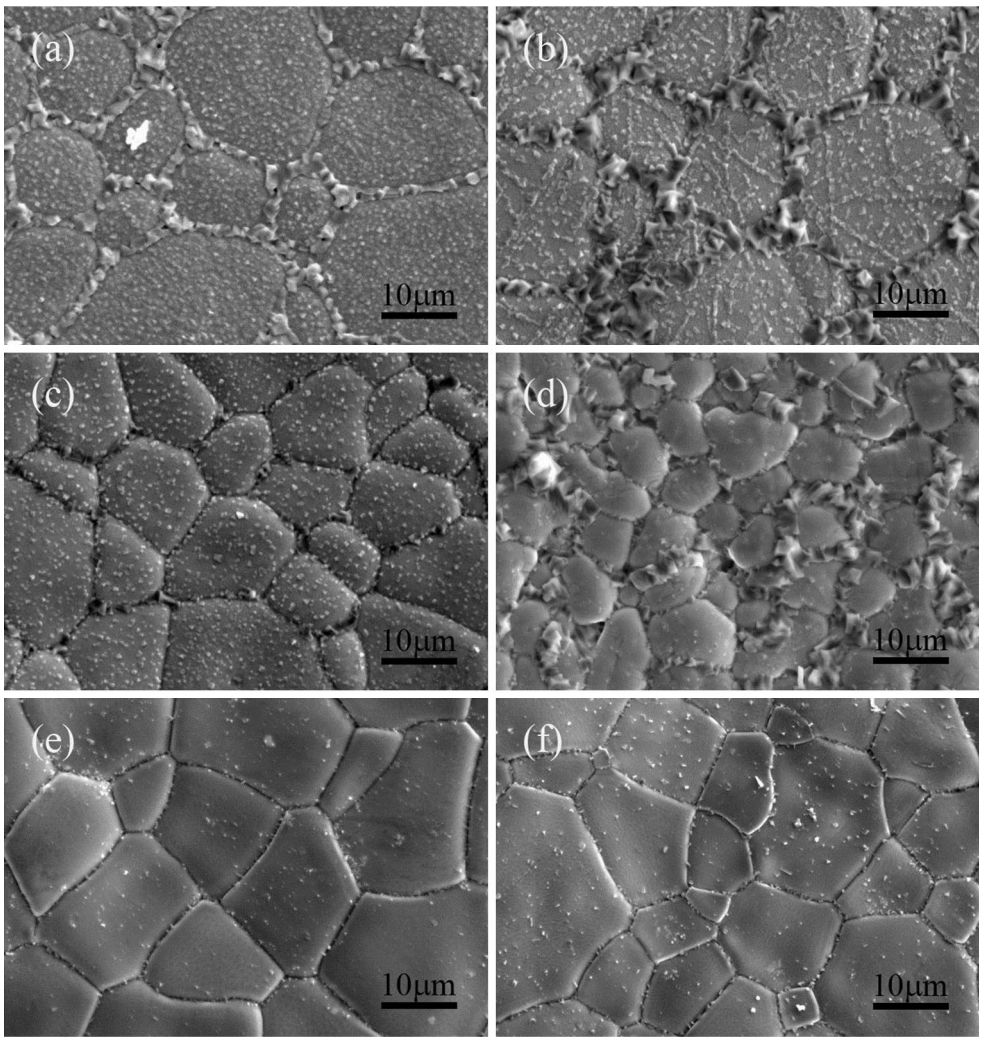

Fig. 4 SEM images of BLCN, BLCFN-0.1, and BLCFN-0.5 membranes after calcining under pure CO_2 at 850 °C for 5 h (*left side*) or 20 h (*right side*)

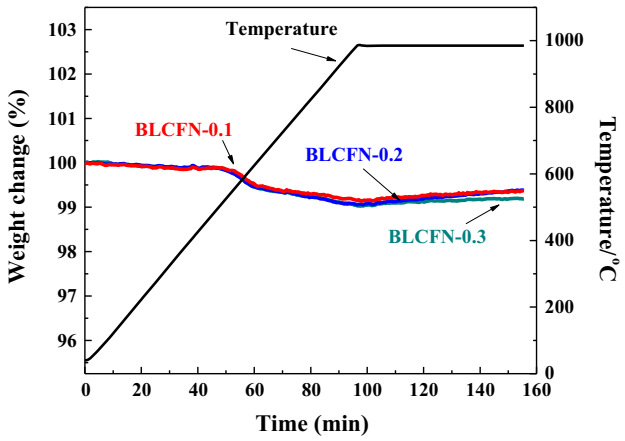

Fig. 5 The weight change of BLCFN powder under CO_2-containing atmosphere. Flowing gas: 50 %CO_2 + 50 %N_2; flowing rate: 20 mL/min

As shown in Fig. 7, with pure He as sweep gas, the oxygen permeability of the BLCFN membranes reaches a stable state at 850 °C after 60 min. When the sweep gas is switched from pure He to CO_2, the oxygen permeation flux for all the BLCFN membranes decreases, but the degree of decline is different. Obviously, the more the doped Fe is, the less the oxygen flux decreases. In addition, after CO_2 is used as the sweep gas, the oxygen fluxes of the BLCFN membranes decreases with the sweeping time. For instance, the oxygen permeation flux of the membrane of BLCFN-0.0 decreased from 1.1 to 0.35 mL cm^{-2} min^{-1} after pure CO_2 is introduced, then to zero after 500 min. However, for the membrane of BLCFN-0.5, at the same condition, the oxygen permeation flux changes from 0.27 to 0.19 mL cm^{-2} min^{-1} firstly, and then to 0.11 mL cm^{-2} min^{-1}.

After oxygen permeation with CO_2 sweeping, Fig. 8 shows the XRD patterns of permeate side of the BLCFN

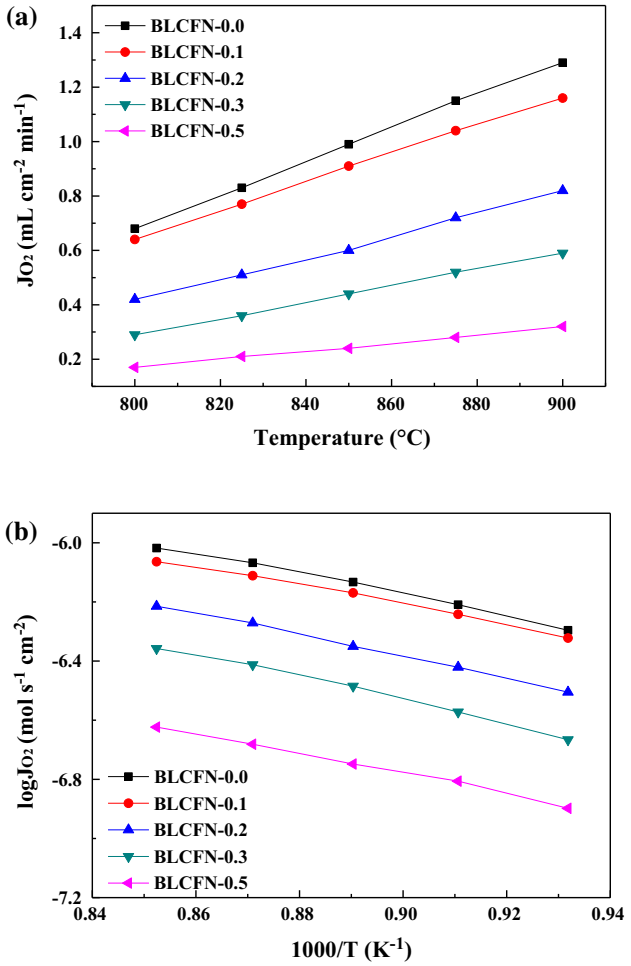

Fig. 6 Temperature dependence of oxygen permeable flues through the BLCFN membranes with different Fe-doping content (**a**), and related Arrhenius plots (**b**). Conditions: 110 mL/min air as feed gas, 80 mL/min He as sweep gas. Membrane thickness: 1.0 mm

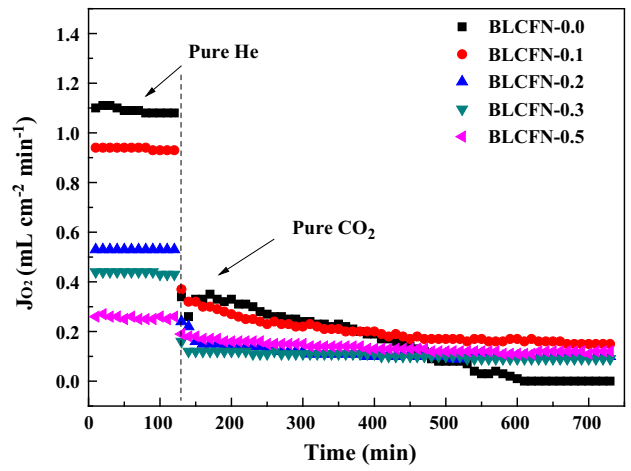

Fig. 7 The oxygen permeation flues of BLCFN material swept by pure CO_2 at 850 °C. Conditions: $F_{He} + F_{CO2} = 80$ mL/min, $F_{air} = 110$ mL/min, thickness = 1.0 mm

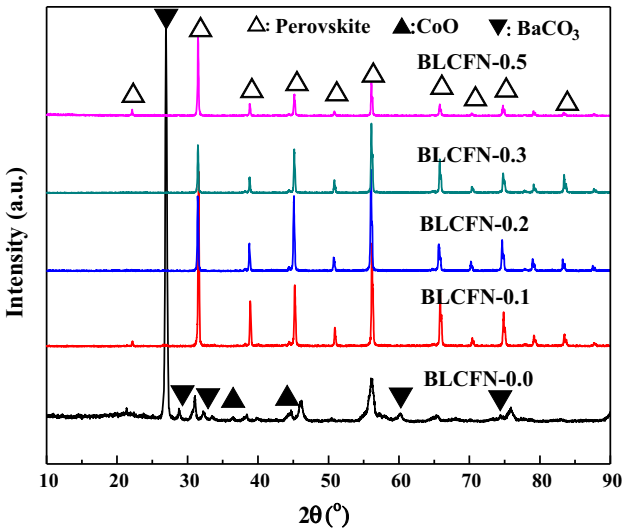

Fig. 8 XRD patterns of permeate side of BLCFN membranes after oxygen permeation measurement at 850 °C for 10 h using pure CO_2 as sweep gas. $BaCO_3$: JCPDS 41-0373; CoO: JCPDS 43-1004; Perovskite: JCPDS 46-0997

membranes after oxygen permeation measurement at 850 °C for 10 h using pure CO_2 as sweep gas. As shown in Fig. 8, the perovskite structure of the BLCFN-0.0 membrane was severely damaged, barium carbonate, and cobalt oxide phases can be observed. It is worthy of noting that, for the Fe-doped BLCFN membranes, the perovskite structure maintains unchanged after oxygen permeation with CO_2 sweeping.

Oxygen permeation results showed that oxygen flux decreased obviously with the change of sweep gas from pure He to CO_2 for the Fe-doped BLCFN membranes. However, XRD patterns do not show any new phases of carbonate, which means that the degradation mechanism of BLCFN membrane may not be caused by barium carbonate formation. Tan et al. [16] investigated the oxygen permeation behavior of LSCF hollow fiber membranes with CO_2 as sweep gas and they considered that a sharp drop of oxygen permeation flux should be resulted from the chemisorbed CO_2 on the surface of membrane. Additionally, another explanation for the sharp drop of oxygen flux, particularly for the alkaline earth metal fully occupied at A-site of perovskite oxides, is the formation of a stable carbonate layer ($BaCO_3$ or $SrCO_3$) on the surface or permeate side [5, 17–19]. It is well-acknowledged that oxygen permeation is preceded by the oxygen ions transportation via oxygen vacancies in the perovskite cubic oxide. Hence, CO_2 chemically adsorption must be the negative effect in the oxygen permeation process due to the decrease of oxygen vacancy concentrations. In this study, although there is no stable barium carbonate ($BaCO_3$) or strontium carbonate ($SrCO_3$) observed in the XRD patterns, the oxygen permeation is also suppressed obviously.

For perovskite oxides, in order to obtain high oxygen ionic conductivity, elemental composition with low ABE should be selected [4]. However, to achieve high CO_2 tolerance, elemental composition with high ABE must be chosen. ABE affects both oxygen surface exchange kinetics and the oxygen ionic bulk diffusion. The ABE value can be calculated as follows [20]:

$$\mathrm{ABE} = \frac{1}{12m}\left(\Delta H_{\mathrm{A_mO_n}} - m\Delta H_{\mathrm{A}} - \frac{n}{2}D_{\mathrm{O_2}}\right) + \frac{1}{6m}\left(\Delta H_{\mathrm{B_mO_n}} - m\Delta H_{\mathrm{B}} - \frac{n}{2}D_{\mathrm{O_2}}\right), \quad (2)$$

where $\Delta H_{\mathrm{A_mO_n}}$ and $\Delta H_{\mathrm{A_mO_n}}$ are the standard formation enthalpy of the oxides and ΔH_{A} and ΔH_{B} are the sublimation energy of the elementary substance, $D_{\mathrm{O_2}}$ is the decomposition energy of oxygen. Based on the ABE calculation, we can find that the Fe-doping increases the ABE markedly. The ABE values are −295.3, −297.7, −300.0, −302.3, and −307.0 kJ/mol for the membrane of BLCFN-0.0, BLCFN-0.1, BLCFN-0.2, BLCFN-0.3, and BLCFN-0.5, respectively.

Although the Fe-doping could enhance the tolerance towards CO_2 of the BLCFN membrane, the oxygen permeation flux of the BLCFN membrane is still decreasing with the CO_2 sweeping time at 850 °C. In order to explore the oxygen permeability of BLCFN at 900 °C using CO_2 as the sweep gas, the membrane of BLCFN-0.2 was selected for the oxygen permeation measurement and the results are shown in Fig. 9. It can be seen that the permeation flux is 0.96 mL cm^{-2} min^{-1} at 900 °C with He sweeping. When the sweep gas was switched from He to CO_2, the oxygen permeation flux decrease with time in the first 50 h and then reach a steady state of ~0.31 mL cm^{-2} min^{-1}. The observations indicated that a stable oxygen permeation could be realized by suitable elemental doping in a single perovskite membrane. Similar to other reports, when the sweep gas was shifted back to He, the oxygen permeation flux through the BLCFN-0.2 membrane can be recovered [5, 21–23].

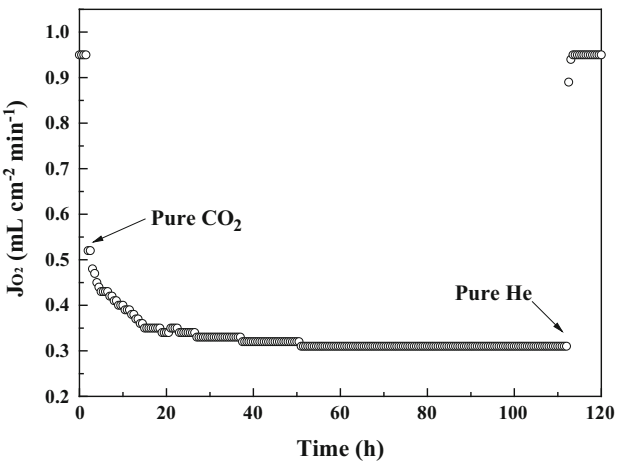

Fig. 9 The oxygen permeation flux of BLCFN-0.2 membrane using pure He and pure CO_2 as sweep gas at 900 °C

Conclusions

Perovskite $Ba_{0.8}La_{0.2}Co_{0.88-x}Fe_xNb_{0.12}O_{3-\delta}$ (BLCFN) powder and membrane were prepared by solid-state reaction and the corrosion behavior of CO_2 on the BLCFN oxide was investigated. Using pure CO_2 as sweep gas, although the oxygen permeation flux of the BLCFN membranes decreases slightly at 850 °C, the degradation becomes less pronounced with increasing content of Fe. The enhanced CO_2 resistance of the perovskite would be result from an increasing ABE due to the Fe-doping. For the membrane which the Fe-doped content equals to 0.2, the oxygen permeation flux is 0.96 mL cm^{-2} min^{-1} at 900 °C with He sweeping. When using pure CO_2 as sweep gas, the oxygen permeation flux decreases slightly in the first 50 h and then reaches a steady state of ~0.31 mL cm^{-2} min^{-1} for more than 60 h in a prolonged continuous oxygen operation.

Acknowledgements We gratefully acknowledge the financial supports from the National Natural Science Foundation of China (Nos. 51274139 and 51174133), Science and Technology Commission of Shanghai Municipality (11ZR1412900), the Innovation Program of Shanghai Municipal Education Commission (13YZ019) and Doctoral Fund of Ministry of Education of China (20123108120020).

References

1. Stadler H, Beggel F, Habermehl M, Persigehl B, Kneer R, Modigell M, Jeschke P (2011) Oxyfuel coal combustion by efficient integration of oxygen transport membranes. Int J Greenh Gas Control 5:7–15
2. Carbo MC, Jansen D, Hendriks C, de Visser E, Jan Ruijg G, Davison J (2009) Opportunities for CO_2 capture through oxygen conducting membranes at medium-scale oxyfuel coal boilers. Energy Procedia 1:487–494
3. Sunarso J, Baumann S, Serra JM, Meulenberg WA, Liu S, Lin YS, Diniz da Costa JC (2008) Mixed ionic–electronic conducting (MIEC) ceramic-based membranes for oxygen separation. J Membr Sci 320:13–41
4. Zhang K, Sunarso J, Shao ZP, Zhou W, Sun CH, Wang SB, Liu SM (2011) Research progress and materials selection guidelines on mixed conducting perovskite-type ceramic membranes for oxygen production. RSC Adv 1:1661–1676
5. Arnold M, Wang HH, Feldhoff A (2007) Influence of CO_2 on the oxygen permeation performance and the microstructure of perovskite-type $(Ba_{0.5}Sr_{0.5})(Co_{0.8}Fe_{0.2})O_{3-\delta}$ membranes. J Membr Sci 293:44–52
6. Yi JX, Schroeder M, Weirich T, Mayer J (2010) Behavior of Ba(Co, Fe, Nb)$O_{3-\delta}$ perovskite in CO_2-containing atmospheres:

degradation mechanism and materials design. Chem Mater 22:6246–6253
7. Chen W, Chen CS, Winnubst L (2011) Ta-doped $SrCo_{0.8}Fe_{0.2}O_{3-\delta}$ membranes: phase stability and oxygen permeation in CO_2 atmosphere. Solid State Ion 196:30–33
8. Zeng Q, Zu YB, Fan CG, Chen CS (2009) CO_2-tolerant oxygen separation membranes targeting CO_2 capture application. J Membr Sci 335:140–144
9. Yi J, Brendt J, Schroeder M, Martin M (2012) Oxygen permeation and oxidation states of transition metals in (Fe, Nb)-doped $BaCoO_{3-\delta}$ perovskites. J Membr Sci 387–388:17–23
10. Yi JX, Schroeder M, Martin M (2013) CO_2-tolerant and cobalt-free SrFe0.8Nb0.2O3-delta perovskite membrane for oxygen separation. Chem Mater 25:815–817
11. Klande T, Ravkina O, Feldhoff A (2013) Effect of A-site lanthanum doping on the CO_2 tolerance of $SrCo_{0.8}Fe_{0.2}O_{3-\delta}$ oxygen-transporting membranes. J Membr Sci 437:122–130
12. Zhang X, Wu C, Zhou J, Yang G, Liu Y, Zhang Y, Ding W (2015) Oxygen permeation property and structural stability of La-doped $BaCo_{0.88}Nb_{0.12}O_{3-\delta}$ membranes in CO_2 atmosphere. Chem J Chin Univ 36:1246–1253
13. Wu C, Gai Y, Zhou J, Tang X, Zhang Y, Ding W, Sun C (2015) Structural stability and oxygen permeability of $BaCo_{1-x}Nb_xO_{3-\delta}$ ceramic membranes for air separation. J Alloys Compd 638:38–43
14. Geng Z, Ding WZ, Wang HH, Wu CZ, Shen PJ, Meng XY, Gai YQ, Ji FT (2012) Influence of barium dissolution on microstructure and oxygen permeation performance of $Ba_{1.0}Co_{0.7}Fe_{0.2}Nb_{0.1}O_{3-\delta}$ membrane in aqueous medium. J Membr Sci 403:140–145
15. Wu CZ, Wang H, Zhang XX, Zhang YW, Ding WZ, Sun CH (2014) Microstructure evolution and oxidation states of Co in perovskite-type oxide $Ba_{1.0}Co_{0.7}Fe_{0.2}Nb_{0.1}O_{3-\delta}$ annealed in CO_2 atmosphere. J Energy Chem 23:575–581
16. Tan XY, Liu N, Meng B, Sunarso J, Zhang K, Liu SM (2012) Oxygen permeation behavior of $La_{0.6}Sr_{0.4}Co_{0.8}Fe_{0.2}O_3$ hollow fibre membranes with highly concentrated CO_2 exposure. J Membr Sci 389:216–222
17. Yang Q, Lin YS, Bulow M (2006) High temperature sorption separation of air for producing oxygen-enriched CO_2 stream. AIChE J 52:574–581
18. Czuprat O, Arnold M, Schirrmeister S, Schiestel T, Caro J (2010) Influence of CO_2 on the oxygen permeation performance of perovskite-type $BaCo_xFe_yZr_zO_{3-\delta}$ hollow fiber membranes. J Membr Sci 364:132–137
19. Tong JH, Yang WS, Zhu BC, Cai R (2002) Investigation of ideal zirconium-doped perovskite-type ceramic membrane materials for oxygen separation. J Membr Sci 203:175–189
20. Sammells AF, Cook RL, White JH, Osborne JJ, MacDuff RC (1992) Rational selection of advanced solid electrolytes for intermediate temperature fuel cells. Solid State Ion 52:111–123
21. Luo HX, Jiang HQ, Klande T, Liang FY, Cao ZW, Wang HH, Caro J (2012) Rapid glycine-nitrate combustion synthesis of the CO_2-stable dual phase membrane $40Mn_{1.5}Co_{1.5}O_{4-\delta}$ -$60Ce_{0.9}Pr_{0.1}O_{2-\delta}$ for CO_2 capture via an oxy-fuel process. J Membr Sci 423:450–458
22. Zheng Q, Xue J, Liao Q, Wei YY, Li Z, Wang HH (2013) CO2-tolerant alkaline-earth metal-free single phase membrane for oxygen separation. Chem Eng Sci 101:240–247
23. Luo HX, Klande T, Cao ZW, Liang FY, Wang HH, Caro J (2014) A CO_2-stable reduction-tolerant Nd-containing dual phase membrane for oxyfuel CO_2 capture. J Mater Chem A 2:7780–7787